Raman scattering study of $KFeF_4$

1992 J. Phys.: Condens. Matter 4 1023

(http://iopscience.iop.org/0953-8984/4/4/013)

J. Phys.: Condens. Matter 4 (1992) 1023–1037. Printed in the UK

Raman scattering study of $KFeF_4$

A Désert, A Bulou and J Nouet

Laboratoire de Physique de l'Etat Condensé, Unité de Recherche Associée au CNRS no 807, Faculté des Sciences, Université du Maine 72017, Le Mans Cédex, France

Received 12 July 1991, in final form 30 September 1991

Abstract. The layered compound $KFeF_4$ that exhibits a structural phase transition at $T_c \simeq$ 380 K from *Bmmb* symmetry (phase I) to *Pcmn* symmetry (phase II) is studied as a function of temperature by polarized Raman scattering. All the Raman lines are attributed on the basis of (i) symmetry analysis of the normal modes of vibration in the aristotype phase (phase I) and the compatibilities relations with the symmetries in phase II; (ii) comparison with $RbFeF_4$ in which the phonon spectrum can be calculated. The phase transition is clearly associated with a soft mode but a residual Raman signal is still observed above T_c; this is attributed to the existence of a disordered phase. Two additional modes exhibit a soft behaviour connected with a (virtual) martensitic transformation.

1. Introduction

$KFeF_4$ is a layered compound consisting of FeF_6 octahedra sheets separated by potassium ions (figures 1(*a*) and 2). Unlike most of the AMF_4 compounds where the octahedra of the successive sheets are superimposed (figure 1(*b*)), in $KFeF_4$ there is a staggered stacking. Since the first description of the structure by Heger *et al* (1971), $KFeF_4$ has been the object of two kinds of studies concerning the following. (i) The magnetic properties in relation to the two-dimensional character and the antiferromagnetic ordering which appears below $T_N = 137$ K. These experiments have mainly been performed by Mössbauer spectroscopy (Heger and Geller 1972, Keller and Savic 1983, Slivka *et al* 1984, Chadwick *et al* 1988) and by neutron scattering (Désert *et al* 1991). (ii) The structural phase transitions (SPT) (Hidaka *et al* 1979, Maciel and Ryan 1981). Hidaka *et al* (1979) found two SPTs at 563 K and 368 K but the more recent work (Désert 1990, Sciau and Grébille 1989) only confirms the low temperature one. The space groups are *Bmmb* (Phase I) and *Pcmn* (Phase II) above and below $T_c = 380$ K respectively: this transition mainly arises from FeF_6 octahedra rotation around the [001] axis. The *Bmmb* symmetry is the highest symmetry for this structural arrangement, that is at high temperature, $KFeF_4$ exhibits the aristotype structure. It must be noted, however, that from group theory consideration Saint-Grégoire and Pérez (1983) predicted the additional existence of an incommensurate phase that might take place (in a small temperature range) between phase I and phase II. Up to now there is no unambiguous experimental evidence for such a phase.

0953-8984/92/041023 + 15 $04.50

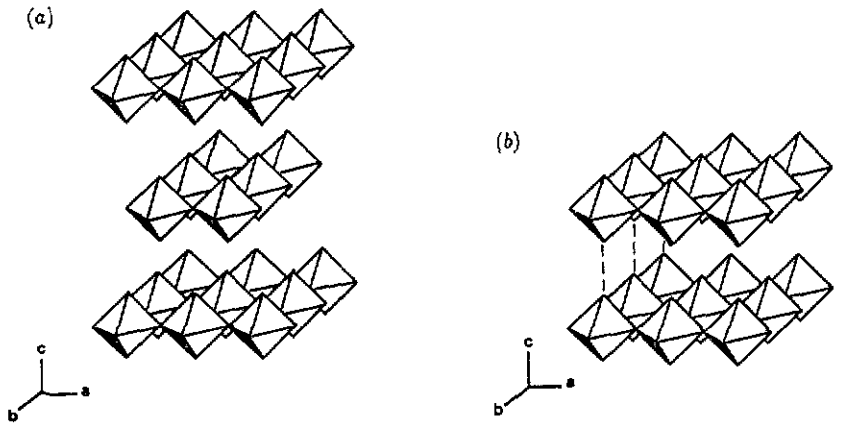

Figure 1. *Octahedra sheets arrangement in $KFeF_4$ (a) and in $TlAlF_4$ (b).*

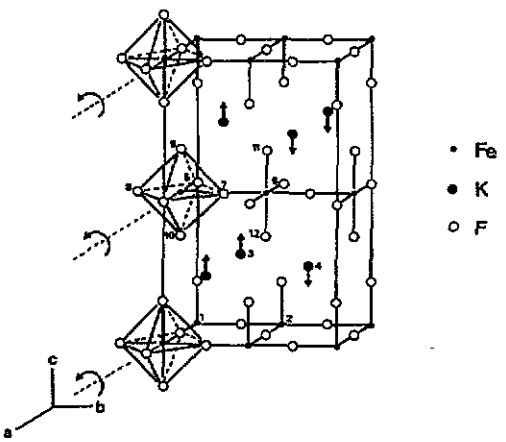

Figure 2. Aristotype structure of $KFeF_4$ (*Bmmb* symmetry). The arrows represent additional octahedra tilts and potassium displacements consistent with the aristotype symmetry. The numbers correspond to the ions labelling used in the text and in the tables.

$KFeF_4$ is also interesting as a reference to study the martensitic transformations encountered in this structural arrangement. Such transitions have been evidenced in $KAlF_4$ (Launay *et al* 1985) and in the mixed compounds $K_{1-x}Rb_xAlF_4$ (Launay *et al* 1987). These compounds, in which the octahedra sheets are superimposed ($TlAlF_4$ type structure) undergo, at low temperature, a shear transition leading to the $KFeF_4$ type structure. In $KAlF_4$ it has been shown that the transition is preceded by the softening of a flat phonon branch and a model has been proposed to establish the relation between the transition and the atomic displacements corresponding to the soft mode (Bulou *et al* 1989a). At the transition the crystal irreversibly breaks and the reverse transition (which is observed with about 90 K hysteresis on warming up the sample) cannot be studied on a single crystal. The investigation of the lattice dynamics properties of an isostructural compound such as $KFeF_4$ which can be prepared as a single crystal and exhibits the aristotype structure, is expected to bring information about the mechanism of the reverse transition. The present work concerns the Raman scattering study. In spite of the high symmetry there is a great number of Raman active modes. An attribution in the absence of a model for the calculation of the phonon spectrum could be difficult. However, in

Table 1. Raman tensors in D_{2h} symmetry.

A_g $\begin{vmatrix} a & - & - \\ - & b & - \\ - & - & c \end{vmatrix}$	B_{1g} $\begin{vmatrix} - & d & - \\ d & - & - \\ - & - & - \end{vmatrix}$	B_{2g} $\begin{vmatrix} - & - & e \\ - & - & - \\ e & - & - \end{vmatrix}$	B_{3g} $\begin{vmatrix} - & - & - \\ - & - & f \\ - & f & - \end{vmatrix}$

these layer compounds many of the vibrational modes correspond to what can be called 'internal modes' of the sheets. Such information is now available from the study of $RbFeF_4$ ($TlAlF_4$ type structure) in which both the Raman scattering study and the calculation of the phonon spectrum (Pique *et al* 1990) have been performed.

2. Experimental procedure

$KFeF_4$ single crystals were prepared at the Laboratoire de Physique de l'Etat Condensé by the Bridgman Stockbarger technique in a platinum crucible. Crystals up to 200 mm^3 have been obtained.

The Raman scattering spectra are collected with a DILOR Z 24 Raman spectrometer. In the temperature range 143 K to 473 K the experiments have been performed (in the back-scattering geometry) under a microscope (BHT Olympus) equipped with a heating and cooling stage CHAIX-MECA. At lower temperatures the experiments were performed by macro-Raman scattering in the classical 90° geometry on a single crystal of 36 mm^3 cut after orientation by x-ray diffraction. The cooling system consisted of a cryo-cooler, and the sample was placed under secondary vacuum. The 514.5 nm and 457.9 nm lines of an argon ion laser Innova 90.3 were used as the exciting source. While 500 mW laser power can be used at room temperature, above 473 K the samples are quickly damaged at much lower laser power. Such a phenomenon has already been observed in $RbFeF_4$.

3. Results

Owing to the large number of modes and the possibility of accidental degeneracy for modes with different symmetries the experimental results are analysed in connection with the predictions of the Raman spectra.

3.1. Phase I

3.1.1. Group theory. In phase I $KFeF_4$ belongs to the *Bmmb* space group with $Z = 2$ formula units per primitive cell†. From group theory the 36 vibrational modes at the centre of the Brillouin zone can be classified according to the D_{2h} irreducible representations as follows

$$4A_g + B_{1g} + 3B_{2g} + 4B_{3g} + 3A_u + 8B_{1u} + 8B_{2u} + 5B_{3u}.$$

A total of 12 Raman active modes is expected. The Raman tensors are given in table 1.

† The choice of this space group (instead of *Cmcm*—the standard one—or *Amma*) makes it easier to connect the vibrations in the $KFeF_4$ structure and the $TlAlF_4$ structure.

Table 2. Symmetry coordinates (x, y, z) relative to the vibrational modes at the centre of the Brillouin zone ($\Gamma(000)$) in phase I of $KFeF_4$.

Modes \ Atoms	1	2	3	4	5	6	7	8	9	10	11	12
Γ_1–A_g	000	000	00a	00$-a$	000	000	00b	00$-b$	0cd	0$-c-d$	0$-cd$	0$c-d$
Γ_3–B_{2g}	000	000	a00	$-a$00	000	000	b00	$-b$00	c00	$-c$00	c00	$-c$00
Γ_5–B_{3g}	000	000	0a0	0$-a$0	000	000	0b0	0$-b$0	0cd	0$-c-d$	0$c-d$	0$-cd$
Γ_7–B_{1g}	000	000	000	000	000	000	000	000	a00	$-a$00	$-a$00	a00
Γ_2–A_u	a00	a00	000	000	b00	$-b$00	000	000	c00	c00	$-c$00	$-c$00
Γ_4–B_{2u}	0ab	0$a-b$	0c0	0c0	0de	0$c-e$	0f0	0f0	0gh	0gh	0$g-h$	0$g-h$
Γ_6–B_{3u}	a00	a00	b00	b00	c00	c00	d00	d00	e00	e00	e00	e00
Γ_8–B_{1u}	0ab	0$-ab$	00c	00c	0de	0$-de$	00f	00f	0gh	0gh	0$-gh$	0$-gh$

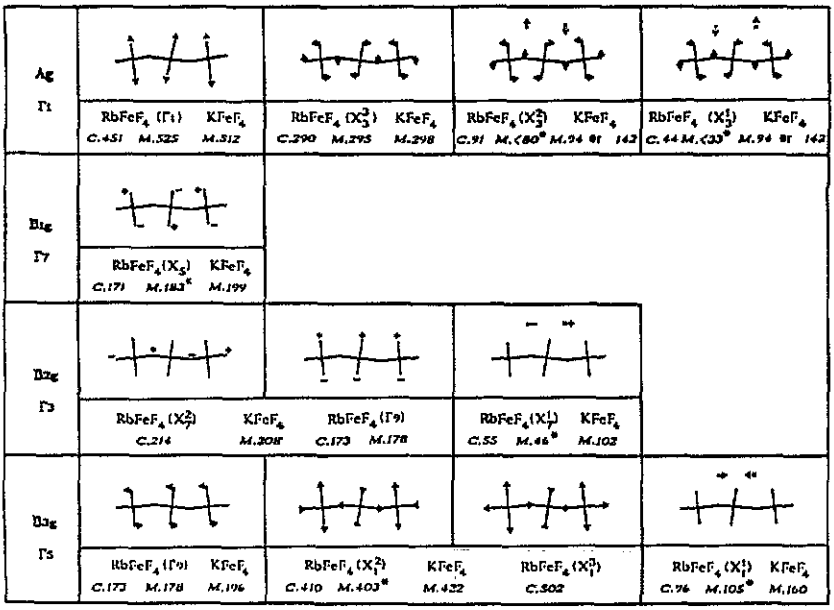

Figure 3. Frequencies in cm^{-1} and normal coordinates of vibration corresponding to the Raman lines observed in $KFeF_4$, with their associated symmetry in $RbFeF_4$ ($TlAlF_4$ type structure) (C: calculated, M: measured at room temperature (*) or at $T = 423$ K).

The symmetry coordinates relative to these modes calculated with the projection operators (Maradudin and Vosko 1968) are reported in table 2. The ions are labelled according to figure 2. Actually, as appeared from the study of the vibrational properties of the $TlAlF_4$ type structure (Bulou *et al* 1989b) in such layered structures the dispersion along the direction normal to the sheets is small. Then, many normal modes can be characterized by the vibrations of the atoms of an octahedra sheet (that is 'internal modes') or by vibration of the octahedra sheets with respect to the monovalent cations sheets. Then, for each symmetry adapted eigenvectors some normal modes of vibration can be predicted. They are reported in figure 3 together with their corresponding

Table 3. Calculated phonon frequencies (in cm^{-1}) of $RbFeF_4$ at the Γ, M, X, Z and R points of the tetragonal primitive Brillouin zone.

	Γ_4^i				Γ_{10}^i		
Γ_1	TO	LO	Γ_8	Γ_9	TO	LO	
451	75	118	184	173	71	86	
	389	363			183	188	
	475	562			280	373	
					496	538	

M_1^i	M_3	M_4^i	M_5	M_6	M_7	M_9^i	M_{10}^i
404	95	165	409	52	329	81	80
540		468				279	195
							346

X_1^i	X_3^i	X_4^i	X_5	X_6^i	X_7^i	X_8^i
96	44	90	171	204	55	89
410	91	234		206	214	274
502	290	494		434		470

Z_1^i	Z_4^i	Z_8	Z_9^i	Z_{10}^i
89	103	184	54	28
423	374		190	174
	573			277
				496

R_1^i	R_2	R_3^i	R_4^i	R_5	R_6^i	R_7	R_8^i
367	55	107	77	185	56	214	86
497		314	228		177		122
			494		206		283
					415		508

symmetry in the $TlAlF_4$ type structure (Bulou *et al* 1989b); these modes are located whether at the Γ (000) or at the X ($0\frac{1}{2}0$) points of the tetragonal primitive Brillouin zone. Their frequencies have been calculated in the case of $RbFeF_4$ in which some of them have been measured by Raman scattering. These frequencies are shown in figure 3 and table 3.

3.1.2. Attribution of the Raman lines (423 K). The Raman spectra collected at 423 K in different geometries are plotted in figure 4(*a*).

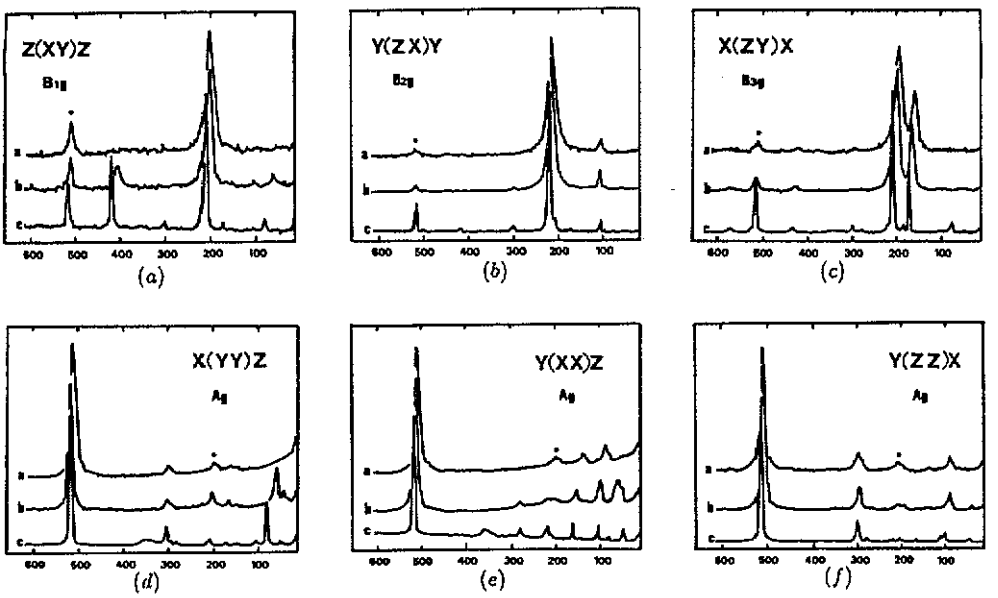

Figure 4. Raman spectra of $KFeF_4$ collected under microscope at 423 K (*a*) and at room temperature (*b*) and Raman spectra performed by macro-Raman (*c*): 95 K (XX); 132 K (ZZ); 110 K (YY); (XY) (ZX) and (ZY). The asterisks denote orientational spill-over of signal from phonons active in other scattering geometry.

(i) *A_g symmetry modes*: Among the four A_g lines the two highest frequencies are expected not to be strongly dependent on the peculiar stacking of $KFeF_4$. Accordingly, two A_g lines are observed at 512 cm^{-1} and 298 cm^{-1} (figure 4) while, from the study of $RbFeF_4$ they are expected in the vicinity of 525 cm^{-1} (Γ_1) and 295 cm^{-1} (X_3^3). The decreasing frequency of the former with respect to $RbFeF_4$ can be obviously explained by the fact that, in $KFeF_4$, the F_{ax} fluorines do not face one another and then the Fe–F_{ax} bond is 'relaxed' (consistent with the Fe–F_{ax} bond length increase (Désert 1990)). The frequencies of the two other A_g symmetry modes (X_3^2 and X_3^1 in $RbFeF_4$) cannot be predicted but they are expected at a lower frequency since they are related to easy octahedra rotations around the [100] axis together with potassium translations along [001]. In $KFeF_4$ two A_g lines are indeed observed at 142 cm^{-1} and 94 cm^{-1}. As discussed later these two modes undergo a significant softening on heating.

(ii) *B_{1g} symmetry modes*: There is only one B_{1g} symmetry line which corresponds to the X_5 mode of the $RbFeF_4$ structure calculated at 171 cm^{-1} and experimentally observed at 183 cm^{-1} at room temperature. Such a prediction is in rather good agreement with the experimental observation in $KFeF_4$ of a B_{1g} symmetry line at 199 cm^{-1}.

(iii) *B_{2g} symmetry modes*: According to figure 3 the two highest frequency modes with B_{2g} symmetry should be related to the X_7^2 and Γ_9 modes calculated at 214 cm^{-1} and 173 cm^{-1} in $RbFeF_4$. The intense line observed at 208 cm^{-1} is consistent with such predictions and should be attributed to the latter which is usually intense. The third B_{2g} line is probably connected with the X_7^1 mode which is calculated and observed in the vicinity of 50 cm^{-1} in $RbFeF_4$. Only the monovalent cations are involved in this mode and it should be expected at a higher frequency in $KFeF_4$ considering the relative mass of potassium with respect to rubidium. The corresponding line in $KFeF_4$ is observed at

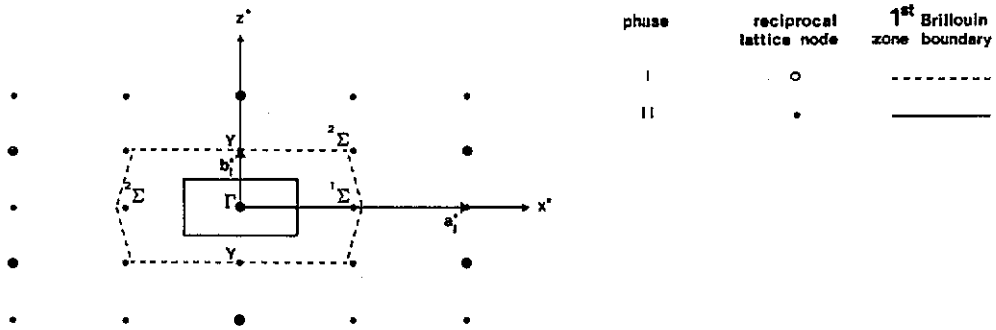

Figure 5. Relation between Brillouin zones of the aristotype phase and phase II.

102 cm^{-1}. The difference is reasonable since the monovalent cations are also expected to be more tightly connected to the sheets in the $KFeF_4$ structure.

(iv) *B_{3g} symmetry modes*: The B_{3g} symmetry modes should be connected with X_1 and Γ_9 modes of $RbFeF_4$. Two of them (X_1^3 and X_1^2) are expected at high frequency (502 and 410 cm^{-1}) while only one is observed at 422 cm^{-1}. The intense line observed at 196 cm^{-1} should be related to the Γ_9 line. Such an attribution is consistent with the observation of a line at 208 cm^{-1} in the B_{2g} symmetry: the degenerated Γ_9 line of the tetragonal $RbFeF_4$ splits in $KFeF_4$ due to the different environment along [100] and [010] axes. The last B_{3g} line at 160 cm^{-1} can be connected with X_1^1 calculated at 96 cm^{-1} in $RbFeF_4$ and arising from monovalent cations displacements along [010] axis. Like the X_1^1 mode in the B_{2g} symmetry, the frequency increase can be explained by the smaller mass of the cation and by the symmetry change.

Hence, the Raman spectra collected in phase I of $KFeF_4$ are in agreement with what can be predicted from the study of $RbFeF_4$. Note, however, that in the A_g symmetry a signal is observed in the frequency range less than about 100 cm^{-1} (figure 4). This will be discussed in section 4. Another signal not strongly temperature dependent may also exist below 20 cm^{-1} (figure 4).

3.2. Phase II

3.2.1. Group theory. The symmetry in phase II is *Pcmn* ($Z = 8$) and the normal modes of vibration at the centre of the Brillouin zone can be classified as follows

$$20A_g + 16B_{1g} + 20B_{2g} + 16B_{3g} + 16A_u + 20B_{1u} + 16B_{2u} + 20B_{3u}$$

that is, 72 modes should be Raman active. For each symmetry a lot of modes are predicted and in this phase they cannot be further distinguished from the group theory point of view. However, as shown in figure 5 the zone centre modes of phase II arise from modes located at $\Gamma(000)$, $Y(001)$, $^1\Sigma(\frac{1}{2}\,0\,0)$ and $^2\Sigma(-\frac{1}{2}\,0\,0)$ points of the aristotype phase I (note that $^1\Sigma$ and $^2\Sigma$ are not high symmetry points but only belong to the $\Sigma(\zeta 00)$ symmetry line).

Modes with the same symmetry in phase II may have different symmetries in phase I where they can be characterized in more detail by group theory alone; the structural phase transition generally does not strongly modify the normal modes of vibration or their frequencies except for the soft modes responsible for the transition. Then, a

symmetry analysis at the Γ, Y, $^1\Sigma$ and $^2\Sigma$ points of phase I associated with the establishment of a compatibility diagram between symmetries in phase I and II can bring more information than the mere analysis in phase II. This compatibility diagram is shown in figure 6 (full lines). The symmetry coordinates at Γ have been reported in table 2 and the symmetry coordinates at Y and Σ are given in tables 4 and 5.

Moreover as we did for phase I, at each of these points the ionic displacements can be connected with the normal mode coordinates of the FeF_6 unit as deduced from the $RbFeF_4$ study. These relationships are reported in figure 6 (dotted lines). While the normal modes at Σ are expected to be closely related to the X_i and M_i modes of $RbFeF_4$, the identification of the Y_i modes is more difficult and probably corresponds to a rough approximation since the R and Z modes should be more dependent on the peculiar stacking especially for the low frequency modes. The relationship is just given as an indication.

Owing to the large number of Raman active modes and the fact that the frequencies in $KFeF_4$ may suffer significant differences with the frequencies calculated in $RbFeF_4$ it cannot be expected to make unambiguously an attribution as in phase I. Moreover, several modes at the Γ, Y, $^1\Sigma$ and $^2\Sigma$ of $KFeF_4$ can be associated to a common mode at the X point of the tetragonal Brillouin zone of $RbFeF_4$ (at the $^1X(0\,\frac{1}{2}\,0)$ and $^2X(\frac{1}{2}\,0\,0)$ points: see the 'horizontal' broken lines in figure 6). Hence, they are expected to have frequencies which are very close, and an overlap of some Raman lines is possible. A similar remark also applies to the modes of $KFeF_4$ related to the degenerated modes Γ_9 and Γ_{10} of $RbFeF_4$ ('vertical' broken lines in figure 6).

3.2.2. Raman spectra in phase II. The Raman spectra collected in phase II in the 90° scattering are shown in figures 4(*b*), (*c*) and the Raman frequencies at room temperature and at the lowest temperature investigated are given in table 6.

In the A_g symmetry, with respect to phase I, at least six additional lines are unambiguously observed (L3, L8, L9, L16, L19, L20); very weak signals (L2, L15) could also be attributed to A_g lines. The L19 line undergoes a marked softening on heating (figures 7 and 8) and can be attributed to the Σ_3/M_3 mode responsible for the transition. The two lines in the vicinity of 280 cm^{-1} (L8 and L9) can be explained by $^2X_3^2$, M_7, $^2X_8^2$, M_{10}^2 or even one of the Γ_{10} modes. The L3 line (and L2 line if any) can be connected with X_8^3 or Γ_{10}^5 (the calculated frequency for modes involving displacements of axial fluorines is always smaller than the experimental one as explained in section 3.1.2.). The two low-frequency L16 and L20 lines can arise from $^2X_3^1$ and $^2X_3^2$ although the absence of a soft character would be more consistent with the low frequency Z_9 and Z_{10} modes, at the extremity of the acoustic phonon branch with wavevector normal to the FeF_6 sheets. Hence, the number of Raman active modes with A_g symmetry is not inconsistent with the prediction even though the L2 and L15 lines exist.

In the B_{1g} symmetry only the L6 line is unambiguously observed which can be reasonably explained by the M_5 or M_1^1 mode.

In the ZX geometry (B_{2g} symmetry) a very weak additional signal (L18) is observed in phase II. This line can be connected with X_1^1 or M_9^1 modes. It must be also noted that the L7 line (A_g symmetry in phase I) seems to be much more intense than in phase I. The contamination by the A_g lines cannot be excluded but such a signal also could arise from the M_9^2 mode which is expected at the same frequency as the X_3^3. Such a hypothesis is also supported by the observation of the same phenomenon in the B_{3g} symmetry (figure 6).

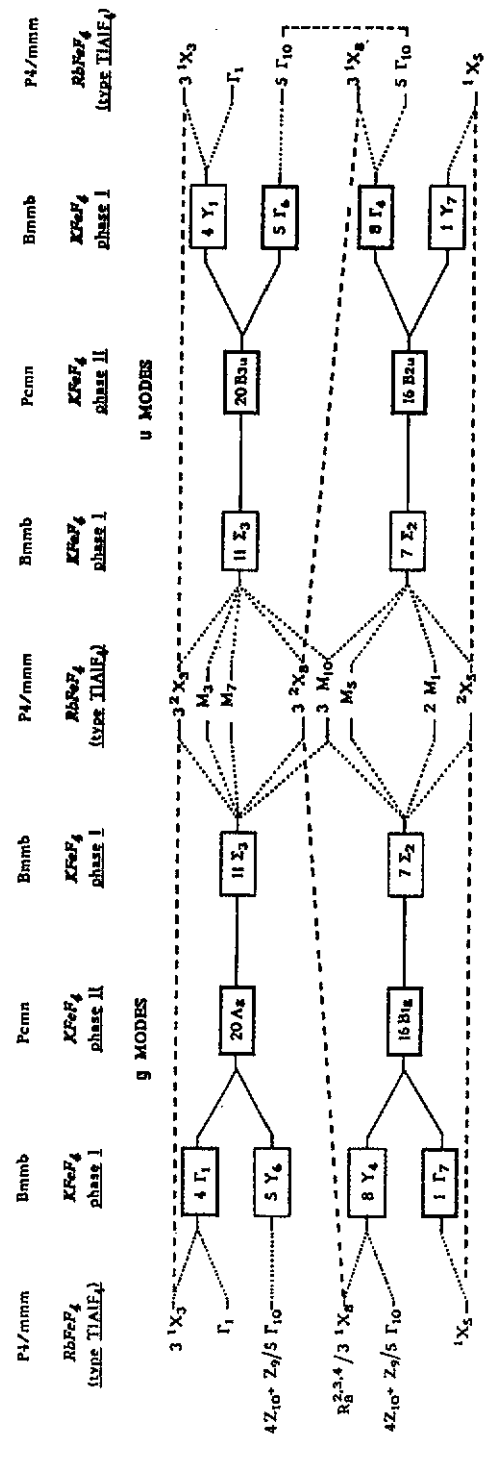

Figure 6. Compatibility diagram between phase I and II of $KFeF_4$ (full line) and relationship between vibrational modes of $RbFeF_4$ and $KFeF_4$ (dotted lines). Broken lines connect two modes with the same frequency in $RbFeF_4$ (at the $^1X(0\,\frac{1}{2}\,0)$ and $^2X(\frac{1}{2}\,0\,0)$ points of the tetragonal $RbFeF_4$ Brillouin zone—'horizontal' broken line—or the two components of a double degenerate mode at the Γ point—'vertical' broken lines) corresponding to four different modes in the $KFeF_4$ structure.

Table 4. Symmetry coordinates (x, y, z) at the Y(0 0 ½) symmetry points.

Modes \ Atoms	1	2	3	4	5	6	7	8	9	10	11	12
Y_2–B_{3g}	$a00$	$a00$	000	000	$b00$	$-b00$	000	000	$c00$	$c00$	$-c00$	$-c00$
Y_4–B_{1g}	$0ab$	$0a-b$	$0c0$	$0c0$	$0de$	$0c-e$	$0f0$	$0f0$	$0gh$	$0gh$	$og-h$	$0g-h$
Y_6–A_g	$a00$	$a00$	$b00$	$b00$	$c00$	$c00$	$d00$	$d00$	$e00$	$e00$	$e00$	$e00$
Y_8–B_{2g}	$0ab$	$0-ab$	$00c$	$00c$	$0de$	$0-de$	$00f$	$00f$	$0gh$	$0gh$	$0-gh$	$0-gh$
Y_1–B_{3u}	000	000	$00a$	$00-a$	000	000	$00b$	$00-b$	$0cd$	$0-c-d$	$0-cd$	$0c-d$
Y_3–B_{1u}	000	000	$a00$	$-a00$	000	000	$b00$	$-b00$	$c00$	$-c00$	$c00$	$-c00$
Y_5–A_u	000	000	$0a0$	$0-a0$	000	000	$0b0$	$0-b0$	$0cd$	$0-c-d$	$0c-d$	$0-cd$
Y_7–B_{2u}	000	000	000	000	000	000	000	000	$a00$	$-a00$	$-a00$	$a00$

In the B_{3g} symmetry two additional lines are unambiguously observed: L1 and L12. The latter can arise from $^2X_7^2$, M_4^1 or even $^2X_4^2$ while the former could be due to $^1X_1^3$, M_4^2, or $^{1,2}X_4^3$.

Hence it appears that the Raman scattering spectra are not inconsistent with what can be predicted on the basis of the compatibility relations and comparison with $RbFeF_4$. The temperature behaviour of the frequencies of these modes is presented in figure 7. Note also that a broad line is observed at low temperature in the vicinity of 350 cm^{-1} in 4c in the Ag symmetry. This line is attributed to the two-magnon scattering resulting from the antiferromagnetic ordering below $T_N = 137$ K.

4. Discussion

4.1. Phase I–phase II structural phase transition

As previously mentioned, the L19 line exhibits a real soft behaviour (figures 7 and 8). As shown by Désert *et al* (1991) and by Sciau and Grébille (1989), the I–II phase transition can be attributed mainly to the condensation of the octahedra libration mode around the [001] axis. Hence the present Raman scattering study evidences the displacive character of the transition and that the L19 line can be attributed to the Σ_3/M_3 mode. As mentioned by St Grégoire and Perez (1983) the symmetry is the same all along the Σ line and there is no peculiar symmetry at the point where the condensation occurs. The transition might be incommensurate. On the other hand such a transition can be described as follows. In these compounds (i) the FeF_6 octahedra are rigid and the phonon branch is expected to harden greatly when the q wavevector is different from $^1\Sigma$ or $^2\Sigma$; (ii) the phonon branch from $^1\Sigma(\frac{1}{2}\,0\,0)$ to $^2\Sigma(\frac{1}{2}\,0\,1)$ is probably flat due to the layer character. Such a transition should be very similar to the phase I–phase II structural phase transition of $RbAlF_4$ and could be explained in a similar way (Bulou *et al* 1990). In this framework the transition is indirect, i.e. the sequence of phases is phase I–phase I′–phase II where phase I′ results from the condensation of the whole phonon branch, $^1\Sigma(\frac{1}{2}\,0\,0)$–$^2\Sigma(\frac{1}{2}\,0\,1)$ in the present case, and exhibits the same symmetry as phase I. The transition observed at T_c corresponds to phase I′–phase II while the virtual transition phase I′–phase I roughly corresponds to the temperature T_L where the square of the soft mode frequency falls to zero. As shown in figure 9, the T_L temperature is close to 550 K: in this framework, the temperature range T_L–T_c corresponds to the disordered phase I′

Table 5. Symmetry coordinates along the $\Sigma(\xi 00)$ symmetry line.

Modes \ Atoms	1	2	3	4	5	6	7	8	9	10	11	12
Σ_1–$B_{2g} + B_{1u}$	*a*00	*a*00	*b*0*c*	*b*0−*c*	*d*00	*d*00	*e*0*f*	*e*0−*f*	*ghi*	*g*−*h*−*i*	*g*−*hi*	*gh*−*i*
Σ_2–$B_{1g} + B_{2u}$	*a*00	−*a*00	0*b*0	0−*b*0	*c*00	−*c*00	0*d*0	0*d*0	*efg*	*e*−*f*−*g*	−*ef*−*g*	−*e*−*fg*
Σ_3–$Ag + B_{3u}$	0*ab*	0−*ab*	*c*0*d*	−*c*0*d*	0*ef*	0−*ef*	*g*0*h*	−*g*0*h*	*ijk*	−*ijk*	*i*−*jk*	−*i*−*jk*
Σ_4–$B_{3g} + A_u$	0*ab*	0−*ab*	0*c*0	0*c*0	0*de*	0*d*−*e*	0*f*0	0*f*0	*ghi*	−*ghi*	−*gh*−*i*	*gh*−*i*

Table 6. Raman line frequencies of $KFeF_4$ in the different geometries at 423 K (phase I) and at the lowest temperatures investigated: 95 K, 110 K or 132 K (phase II).

	Symmetry							
	A_g		B_{1g}		B_{2g}		B_{3g}	
Phase	I	II	I	II	I	II	I	II
Number of lines expected	4	20	1	16	3	20	4	16
Number of lines observed	4	12	1	2	2	3	3	5
L_{20}		49						
L_{19}		79						
L_{18}						97		
L_{17}	94	105			102	106		
L_{16}		112						
L_{15}		150						
L_{14}	142	160						
L_{13}							160	171
L_{12}								185
L_{11}			199	208			196	206
L_{10}					208	219		
L_9		278						
L_8		289						
L_7	298	301						
L_6				418				
L_5							422	432
L_4	512	514						
L_3		555						
L_2		560						
L_1								570

and T_c would correspond to an order–disorder phase transition. The existence of a disordered phase I′ can explain the persistence above T_c of the Raman signal below about 100 cm^{-1}. This signal slowly decreases on warming up the sample and is expected to disappear above T_L. Unfortunately it has not been possible to check this prediction since, as previously mentioned, the samples are quickly damaged above about 473 K.

The temperature T_L, as deduced from the extrapolation of $\omega^2(T)$ is surprisingly close to the temperature 563 K where Hidaka *et al* 1979 observed the disappearance of a diffraction line together with a dielectric anomaly. This transition has never been reported elsewhere. However, and although our description requires additional experimental investigation to be proved, it must be noted that it could explain Hidaka's results: the existence above T_c of a disordered phase induced by the condensation of a flat phonon branch should result in the presence of diffuse scattering lines which may look like a diffraction line when studied on a single crystal; such a diffuse scattering signal should disappear at T_L.

Of course, additional experimental investigations (x-ray diffuse scattering or inelastic neutron scattering) are required to prove unambiguously the existence of an intermediate disordered phase I′. Moreover, it would be important to compare the frequencies in phase II of the modes at the edges of the phonon branch that condenses. One of these modes has been measured by Raman scattering ($^1\Sigma_3/M_3$) while the other ($^2\Sigma_3/M_3$) could be measured by infra-red spectroscopy since it has B_{3u} symmetry. The

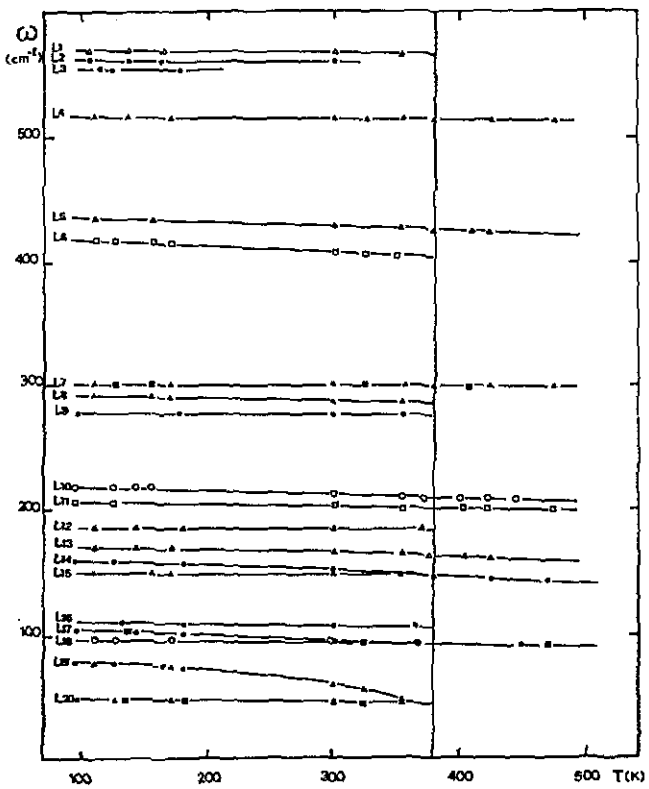

Figure 7. Temperature behaviour of the Raman active mode frequencies. The full symbols correspond to the XX (circles), YY (triangles) and ZZ (squares) geometries. The open circles correspond to the XY geometries, open triangles to YZ and the open squares to XY geometries. Full lines are only guides for the eyes. The vertical line represents the transition temperature.

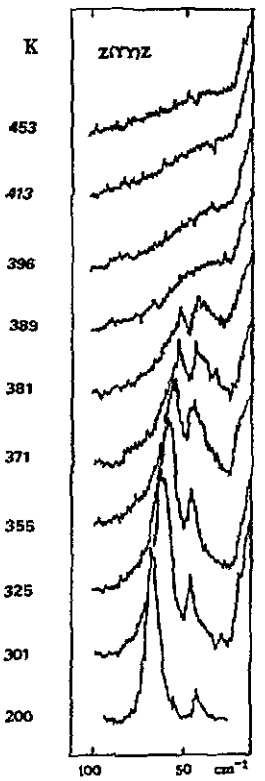

Figure 8. Temperature dependence of the L19 Raman line.

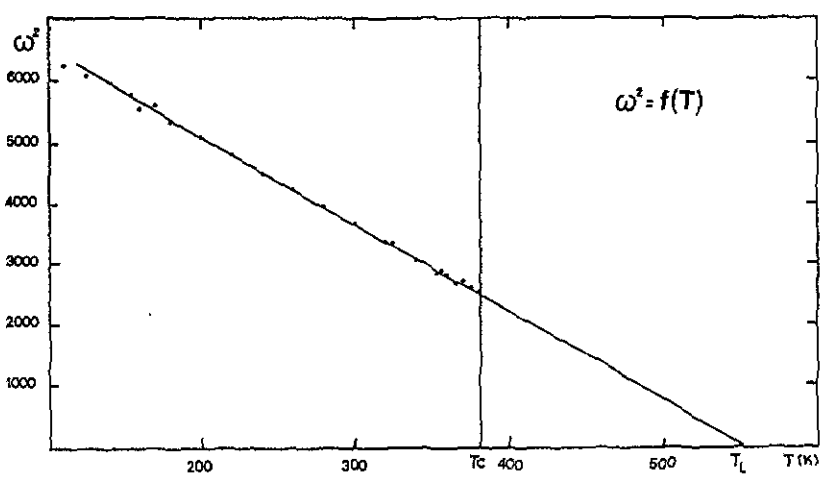

Figure 9. Square of the frequency of the soft mode (L19 line) as a function of temperature.

uncommon fact that the two extremities of a (probably) quasi-flat phonon branch corresponding to octahedra librations give rise to a Raman active mode and an infrared active mode comes from the (uncommon) fact that in phase II there is no symmetry centre at the centre of the octahedra (Désert *et al* 1991).

4.2. Martensitic transition

As shown by Bulou (1985) these layer structures may undergo martensitic transformations as occurs in metallic alloys. Such a transformation is observed in the vicinity of 260 K in potassium tetrafluoroaluminate $KAlF_4$ which exhibits the $TlAlF_4$ type structure at high temperature and the $KFeF_4$ type structure at low temperature (Launay *et al* 1985). In the high-temperature phase the transition is preceded by the softening of the quasi-flat zone boundary phonon branch from X_3^1 to M_5^1. It has been shown that the transition can be explained by the condensation of the X_3^1 mode which weakens the octahedra sheets clamping achieved by the potassium ions (Bulou *et al* 1989a). In this framework the reverse transition from the $KFeF_4$ structure to the $TlAlF_4$ structure which occurs in the vicinity of 363 K is expected to be also preceded by the softening of the modes corresponding to X_3^1. Although such a transition is not observed in $KFeF_4$, it is expected to be inherent in the structure and a softening is expected on heating this sample. These modes are the two low frequency A_g modes at the centre of the Brillouin zone of $KFeF_4$ aristotype structure (L14 and L17). Although not drastic, a significant softening of these two modes is observed (figure 7). This result supports the hypothesis of the existence of an additional phase transition in $KFeF_4$ if the melting point were (much) higher. Since phase I is the highest symmetry for the $KFeF_4$ structural arrangement, such a transition would be reconstructive, presumably similar to the martensitic transformation of $KAlF_4$.

5. Conclusion

The Raman spectra of $KFeF_4$ which contain a large number of lines have been investigated in detail on the basis of group theory and by comparison with $RbFeF_4$. All the Raman lines have been attributed in phase I while in phase II it has been shown that the spectra are not inconsistent with what can be predicted. It must be emphasized that in such layered materials the attribution can be performed in terms of the internal modes characteristic of the FeF_6 sheets. This study completes the data about the dynamics of FeF_6 vibrations obtained in $RbFeF_4$. Such information can be used for electron–phonon interactions studies (Ducouret-Cereze and Varret 1988).

It has been shown that the structural phase transition at $T_c = 380$ K is related to the condensation of a soft mode located along the Σ line inside the Brillouin zone of the aristotype phase. As in $RbAlF_4$, such a transition could be explained in terms of an indirect transition phase I–phase I′–phase II where the intermediate phase I′, which extends from T_c to $T_c + 130$ K, would be disordered. This could explain the Raman signal observed at low frequency above T_c. To confirm this interpretation it would be necessary to investigate the phonon spectrum by inelastic neutron scattering; note that in this structure the soft mode in phase II could also be studied by infra-red spectroscopy. It must be pointed out that one of the main problems in proving unambiguously the existence of an intermediate phase I′ in $RbAlF_4$ is due to the fact that the transition occurs at a high temperature and so the soft mode cannot be studied over a large

temperature range. It would be easier in $KFeF_4$ as the transition occurs at a significantly lower temperature.

The additional significant softening of two A_g symmetry modes has been observed in the whole temperature range investigated. We attribute this behaviour to a (virtual) martensitic transition that would occur at high-temperature (above the melting point). Such a softening is expected in the quasi-isomorphous $KAlF_4$ that undergoes a martensitic transition but that cannot be grown as a single crystal in its low temperature phase. The present attribution of the Raman lines on $KFeF_4$ single crystals should be useful in investigating the Raman spectra of $KAlF_4$.

Acknowledgments

The authors wish to thank G Niesseron for the preparation of the crystal sample and Professor M Rousseau for his advice in the Raman scattering experiments.

References

Bulou A 1985 *PhD Thesis* Université du Maine
Bulou A, Gibaud A, Launay C, Debieche M, Rousseau M, Nouet J and Hennion B 1989a *Phase Transitions* **14** 47–53
Bulou A, Rousseau M, Nouet J and Hennion B 1989b *J. Phys. Condens. Matter* **1** 4553
Bulou A, Rousseau M and Nouet J 1990 *Ferroelectrics* **104** 373
Chadwick J, Thomas M F, Johnson C E and Jones D H 1988 *J. Phys. C: Solid State Phys.* **21** 6159
Désert A 1990 *PhD Thesis* Université du Maine
Désert A, Bulou A, Leblanc M and Nouet J 1991 in preparation
Ducouret-Céreze A and Varret F 1988 *J. Physique* **49** 661
Heger G, Geller R and Babel D 1971 *Solid State Commun.* **9** 335
Heger G and Geller R 1972 *Phys. Status. Solidi* b **53** 227
Hidaka M, Garrard B J and Wanklyn B M R 1979 *J. Phys. C: Solid State Phys.* **12** 2737
Keller H and Savic I M 1983 *Phys. Rev.* B **28** 2638
Launay C, Bulou A and Nouet J 1987 *Solid State Commun.* **69** 539
Launay J M, Bulou A, Hewat A N, Gibaud A, Laval J Y and Nouet J 1985 *J. Physique* **46** 771
Maciel A and Ryan J F 1981 *J. Physique Coll. Suppl.* **42** C6 716
Maradudin A A and Vosko S M 1968 *Rev. Mod. Phys.* **40** 1–37
Pique C, Bulou A, Moron M C, Burriel R, Fourquet J L and Rousseau M 1990 *J. Phys.: Condens. Matter* **2** 8277
Saint Grégoire P and Pérez A 1983 *Z. Krist.* **163** 135
Sciau Ph and Grébille D 1989 *Phys. Rev.* B **39** 11982
Slivka J, Keller H, Kundig W and Wanklyn B M 1984 *Phys. Rev.* B **30** 3649